

## ON THE REDSHIFT OF TEV BL LAC OBJECTS

SIMONA PAIANO<sup>1,2</sup>, MARCO LANDONI<sup>2</sup>, RENATO FALOMO<sup>1</sup>, ALDO TREVES<sup>3</sup>, RICCARDO SCARPA<sup>4</sup>, CHIARA RIGHI<sup>2,3</sup>

<sup>1</sup>INAF, Osservatorio Astronomico di Padova, Vicolo dell'Osservatorio 5 I-35122 Padova (PD) - ITALY

<sup>2</sup>INAF, Osservatorio Astronomico di Brera, Via E. Bianchi 46 I-23807 Merate (LC) - ITALY

<sup>3</sup>Università degli Studi dell'Insubria, Via Valleggio 11 I-22100 Como - ITALY

<sup>4</sup>Instituto de Astrofísica de Canarias, C/O Via Lactea, s/n E38205 - La Laguna (Tenerife) - ESPANA

### ABSTRACT

We report results of a spectroscopic campaign carried out at the 10 m Gran Telescopio Canarias for a sample of 22 BL Lac objects detected (or candidates) at TeV energies, aimed to determine or constrain their redshift. This is of fundamental importance for the interpretation of their emission models, for population studies and also mandatory to study the interaction of high energy photons with the extragalactic background light using TeV sources. High signal-to-noise optical spectra in the range 4250 - 10000 Å were obtained to search for faint emission and/or absorption lines from both the host galaxy or the nucleus. We determine a new redshift for PKS 1424+240 ( $z = 0.604$ ) and a tentative one for 1ES 0033+595 ( $z = 0.467$ ). We are able to set new spectroscopic redshift lower limits for other three sources on the basis of Mg II and Ca II intervening absorption features: BZB J1243+3627 ( $z > 0.483$ ), BZB J1540+8155 ( $z > 0.672$ ), and BZB 0J2323+4210 ( $z > 0.267$ ). We confirm previous redshift estimates for four blazars: S3 0218+357 ( $z = 0.944$ ), 1ES 1215+303 ( $z = 0.129$ ), W Comae ( $z = 0.102$ ), and MS 1221.8+2452 ( $z = 0.218$ ). For the remaining targets, in seven cases (S2 0109+22, 3C 66A, VER J0521+211, S4 0954+65, BZB J1120+4214, S3 1227+25, BZB J2323+4210), we do not validate the proposed redshift. Finally for all sources of still unknown redshift, we set a lower limit based on the minimum equivalent width of absorption features expected from the host galaxy.

*Keywords:* BL Lac object spectroscopy — Redshift — TeV astronomy — Extragalactic Background Light

### 1. INTRODUCTION

Blazars are luminous emitters over the whole electromagnetic spectrum up to TeV energies. They are highly variable and polarized and are often dominated, especially during outbursts, by the gamma-ray emission. The standard paradigm for these sources is that they owe their extreme physical behavior to the presence of a relativistic jet closely aligned with the observers direction, a model that explains most of the peculiar properties of these sources: superluminal motion, rapid variability, huge radio brightness temperature, etc. From the optical point of view, blazars showing very weak lines or a completely featureless spectra are named BL Lac objects (BLLs) (see e.g. the review of Falomo et al. 2014).

Compared to other AGN, the featureless spectrum of BLLs is due to the extreme dominance of the non-thermal emission over the stellar emission of the host

galaxy, which make the assessment of their redshift very difficult. (Sbarufatti et al. 2005b, 2006b,a, 2008; Landoni et al. 2012; Shaw et al. 2013; Landoni et al. 2013, 2014; Massaro et al. 2014, 2015; Landoni et al. 2015; Álvarez Crespo et al. 2016).

The knowledge of the distance is, however, crucial to understand the nature of these sources, the physical mechanism responsible for their extremely energetic emission, their intrinsic luminosity, and cosmic evolution. Furthermore, in the case of TeV BLLs, the simple knowledge of the redshift converts these sources into powerful probe of the Extragalactic Background Light (EBL) through  $\gamma - \gamma$  absorption, also improving our understanding of supersymmetric particles thought to be produced in their ultra-relativistic jet (see e.g. Tavecchio et al. 2015). Thus, we undertook a spectroscopic observational campaign of a sample of TeV (or TeV candidate) BLLs with unknown or uncertain redshift to be observed at the 10.4m Gran Telescopio CANARIAS (GTC), in order to improve our knowledge of the redshift of TeV BLLs, a possibly unique test-bench for ultra-high

energy fundamental physics.

The first results of this program were presented in [Landoni et al. \(2015\)](#) for S4 0954+65 and [Paiano et al. \(2016\)](#) for S2 0109+22. In this paper we report results for 22 additional BLLs: 15 of them detected at TeV energies, while 7 being good TeV candidates ([Massaro et al. 2013](#)).

In Section 2 we outline the selection criteria of our sample and discuss their main properties. In Section 3 we present the data collection and the reduction procedure. In Section 4 we show the optical spectra of each object, underlying their main features, and discuss their redshift. In Section 5 we give detailed notes on individual objects and finally in Section 6 we summarize and discuss the results.

In this work we assume the following cosmological parameters:  $H_0 = 70 \text{ km s}^{-1} \text{ Mpc}^{-1}$ ,  $\Omega_\Lambda=0.7$ , and  $\Omega_m=0.3$ .

## 2. THE SAMPLE

We selected all BLLs that are detected at Very High Energy band (VHE;  $>100 \text{ GeV}$ ) from the online reference catalog of TeV sources (TeVCAT<sup>1</sup>) with unknown or uncertain redshift and that are observable from La Palma ( $\delta > -20^\circ$ ). For objects with uncertain redshift we choose sources with contrasting redshift values reported in literature or with measurements from optical spectra of low signal-to-noise ratio. This selection yields 18 targets and we obtain observations for 15 of them (see Tab.1) that represent about 70% of the whole sample of TeV blazars with uncertain or unknown redshift.

In addition we selected BLLs from a sample of 41 objects<sup>2</sup> proposed as TeV emitters by [Massaro et al. \(2013\)](#) on the basis of the combined IR and X-ray properties of BLLs reported in the ROMA-BZCAT catalog ([Massaro et al. 2009](#)), satisfying the criteria of uncertain redshift and observability. This selection produced 12 TeV candidates and we obtained spectra for 7 of them (see Tab.1) that represent  $\sim 60\%$  of the unknown/uncertain TeV candidate emitters proposed by [Massaro et al. \(2013\)](#). 1424+240

## 3. OBSERVATIONS AND DATA REDUCTION

Observations were obtained between February 2015 and August 2016 in Service Mode at the GTC using the low resolution spectrograph OSIRIS ([Cepa et al. 2003](#)). The instrument was configured with the two grisms R1000B and R1000R<sup>3</sup>, in order to cover the spec-

tral range 4000-10000 Å, and with a slit width = 1'' yielding a spectral resolution  $\lambda/\Delta\lambda = 800$ .

For each grism three individual exposures were obtained (with exposure time ranging from 300 to 1200 seconds each, depending on the source magnitude), that were then combined into a single average image, in order to perform optimal cleaning of cosmic rays and CCD cosmetic defects. Detailed information on the observations are given in Tab.2.

Data reduction was carried out using IRAF<sup>4</sup> and adopting the standard procedures for long slit spectroscopy with bias subtraction, flat fielding, and bad pixel correction. Individual spectra were cleaned of cosmic-ray contamination using the L.A.Cosmic algorithm ([van Dokkum 2001](#)).

Wavelength calibration was performed using the spectra of Hg, Ar, Ne, and Xe lamps and providing an accuracy of 0.1 Å over the whole spectral range. Spectra were corrected for atmospheric extinction using the mean La Palma site extinction table<sup>5</sup>. Relative flux calibration was obtained from the observations of spectrophotometric standard stars secured during the same nights of the target observation. For each object the spectra obtained with the two grisms were merged into a final spectrum covering the whole desired spectral range.

Thanks to the availability of a direct image of the target, which is obtained at GTC as part of target acquisition, the spectra could be flux calibrated. The calibration was assessed using the zero point provided by the GTC-OSIRIS webpage<sup>6</sup>. For half of our sample it was also possible to use stars with known flux from the SDSS survey to double check the flux calibration. We found no significant difference on average between the two methods within  $\sim 0.1 \text{ mag}$ . The final spectra were then calibrated to have the flux at 6231 Å equal to the photometry found for the targets (see Tab. 2). Finally each spectrum has been dereddened, applying the extinction law described in [Cardelli et al. \(1989\)](#) and assuming the E(B-V) values taken from the NASA/IPAC Infrared Science Archive<sup>7</sup>.

## 4. RESULTS

The optical spectra of the targets are presented in Fig. 4. In order to emphasize weak emission and/or absorption features, we show also the normalized spec-

<sup>1</sup> <http://tevcats2.uchicago.edu/>

<sup>2</sup> half of them have unknown or uncertain redshift

<sup>3</sup> <http://www.gtc.iac.es/instruments/osiris/osiris.php>

<sup>4</sup> IRAF (Image Reduction and Analysis Facility) is distributed by the National Optical Astronomy Observatories, which are operated by the Association of Universities for Research in Astronomy, Inc., under cooperative agreement with the National Science Foundation.

<sup>5</sup> <https://www.ing.iac.es/Astronomy/observing/manuals/>

<sup>6</sup> <http://www.gtc.iac.es/instruments/osiris/media/zeropoints.html>

<sup>7</sup> <https://irsa.ipac.caltech.edu/applications/DUST/>

trum. This was obtained by dividing the observed calibrated spectrum by a power law continuum fit of the spectrum, excluding the telluric absorption bands (see Tab. 3). These normalized spectra were used to evaluate the SNR in a number of spectral regions. On average the SNR ranges from 150-200 at 4500 Å and 8000 Å respectively, to a peak of 320 at 6200 Å. See details in Tab. 3 and all these spectra can be accessed at the website <http://www.oapd.inaf.it/zblac/>.

#### 4.1. Search for emission/absorption features

All spectra were carefully inspected to find emission and absorption features. When a possible feature was identified, we determined its reliability checking that it was present on the three individual exposures (see Sec. 3 for details). We were able to detect spectral lines for 9 targets. In particular we observe [O III] 5007 Å weak emission in the spectra of 1ES 1215+303, W Comae, MS 1221.8+2452 and PKS 1424+240, [O II] 3727 Å in 1ES 0033+595, 1ES 1215+303 and PKS 1424+240, the Ca II 3934,3968 Å doublet absorption system and the G-band 4305 Å absorption line in MS 1221.8+2452, a strong emission of Mg II 2800 Å in S3 0218+357 and intervening absorption systems due to Mg II 2800 Å in BZB J1243+3627 and BZB J1540+8155 and, finally the Ca II 3934,3968 Å doublet in the spectrum of BZB J2323+4210. Details in Fig. 5 and Tab. 5. The spectrum of 7 additional targets is found completely featureless even though a redshift is reported in literature. Details about the optical spectra and redshift estimates for each objects of our sample are given in Sec. 5.

#### 4.2. Redshift lower limits

Based on the assumption that all BLLs are hosted by a massive elliptical galaxy (e.g. Falomo et al. 2014) one should be able to detect faint absorption features from the starlight provided that the SNR and the spectral resolution are sufficiently high. In the case of no detection of spectral features it is possible to set a lower limit to the redshift based on the minimum Equivalent Width (EW) that can be measured in the spectrum.

The minimum measurable equivalent width ( $EW_{min}$ ) was set according to the scheme outlined by Sbarufatti et al. (2006a,b), though in a more elaborated procedure (see Appendix A). In brief from the normalized spectrum (see Fig. 4) we computed the nominal EW adopting a running window of 15 Å for five intervals of the spectra that avoid the prominent telluric absorption features (see Tab. 3). The procedure yields for each given interval a distribution of EW and we took as minimum measurable EW three times the standard deviation of the distribution (see details in Appendix A).

Five different intervals were considered because the SNR changes with wavelength. The range of  $EW_{min}$  is

reported in Tab. 3 and we give a lower limit on  $z$  assuming a standard average luminosity for the host galaxy  $M_R = -22.9$  (or  $M_R = -21.9$  in parenthesis).

### 5. NOTES FOR INDIVIDUAL SOURCES

**BZB J0035+1515:** The source was first discovered by Fischer et al. (1998) and catalogued as BLL on the basis of its featureless optical spectrum. A more recent optical spectrum, obtained as part of the SDSS survey, exhibits no features (although the automatic procedure suggests some tentative values, also included in NED). Also Shaw et al. (2013) found a featureless spectrum.

We confirm the featureless nature of the spectrum from 4200 to 9000 Å and from our high SNR we obtain an  $EW_{min}$  of 0.09 - 0.18 Å, which correspond to a redshift lower limit of  $z > 0.55$

**1ES 0033+595:** Perlman et al. (1996) identified this Einstein Slew Survey source as a BLL finding a featureless optical spectrum (although a tentative redshift  $z = 0.086$  was derived by Perlman et al. as mentioned in Falomo & Kotilainen (1999)). In Scarpa et al. (1999) the HST images of this object shows two unresolved sources, “A” and “B”, separated by 1".58 and with magnitude  $m_R = 17.95 \pm 0.05$  and  $18.30 \pm 0.05$  mag respectively. On the basis of radio coordinates the authors identified the source B as the most probable BLL counterpart and A as a possible star.

In our spectrum the two sources are partially resolved (see Fig. 1) and we perform a de-blending during the extraction process in order to obtain two separated spectra for the targets. The spectrum of the object “A” (Fig. 2) shows the typical stellar absorption lines of G stars, confirming the previous classification. For the “B” source we obtain a spectrum with a  $SNR \sim 100$  (see Fig. 4) and although there is some contamination of the spectrum by the companion, the non detection of  $H_\alpha$  indicates that the “B” object has an extragalactic nature and it is the blazar counterpart as proposed by Scarpa et al. (1999). We found an emission feature at 5468 Å of  $EW = 0.4$  Å (see Fig. 5). This feature is detected in all three individual spectra and therefore we consider it a secure detection. If identified as [OII] 3727 Å emission, a tentative redshift of  $z = 0.467$  can be provided.

Finally, comparing our photometry with Scarpa et al. (1999), we obtain the same value for the A object, while for the object B we obtain a magnitude difference of 1.2 with respect to the previous one reinforcing the classification of this source as a BLL.

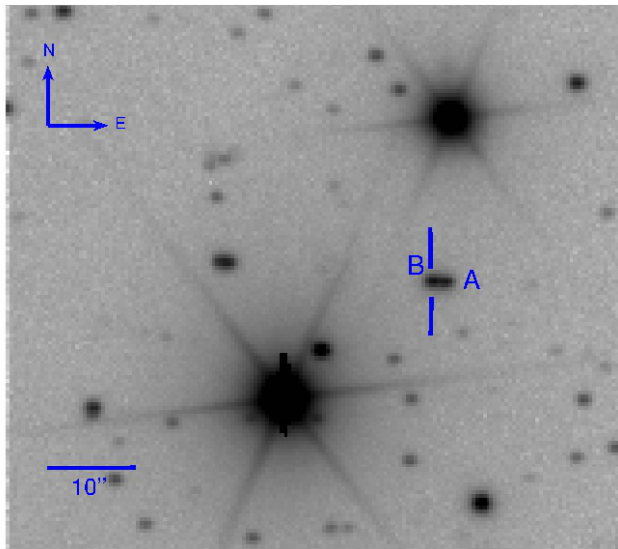


**Figure 1.** r-band optical image of the sky region around the BL Lac object 1ES 0033+595 obtained at the GTC. The source flagged as “A” is a foreground star and the BLL is the source labelled as “B”.

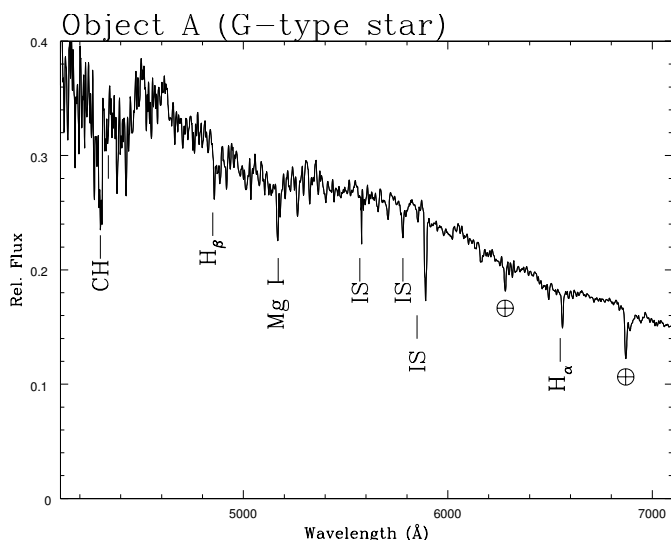


**Figure 2.** GTC spectrum of the companion source, labelled as “A” (see Fig. 1, of the BL Lac object 1ES 0033+595). Absorption lines due to CH (4299 Å), hydrogen (4342 Å, 4863 Å, 6565 Å), and Mg I (5176 Å) are clearly detected. Telluric bands are indicated by ⊕. This object can be classified as a G-type star.

**RGB J0136+391:** The first identification of this source as BLL was proposed by Laurent-Muehleisen et al. (1998) showing a featureless optical spectrum. The same result was found in Wei et al. (1999); Piranomonte et al. (2007) and Shaw et al. (2013). A lower limit on the redshift of  $z > 0.40$  was set on the basis of high quality i-band images obtained at the Nordic Optical Telescope (NOT) (Nilsson et al. (2012)).

We found our high SNR ( $\sim 200$ -480) optical spectrum completely featureless, only allowing to set a lower limit to the redshift of  $z > 0.27$ .

**S3 0218+357:** This source was discovered to be a gravitational lens by Patnaik et al. (1993) who detected two similar radio sources with  $\sim 0.33''$  separation and an Einstein ring with the same diameter. Optical counterparts of the two radio-sources were observed and detected by HST images (Jackson et al. 2000; York et al. 2005). An optical spectrum of the source was obtained by Browne et al. (1993) who detect absorption features of Ca II and Mg II attributed to the lens galaxy at  $z = 0.684$ . They also claim the detection of very weak emission lines of [OII] 3727Å and [OIII] 5007Å. In addition they suggest the presence of weak emission feature of Mg II 2800Å attributed to the blazar proposing a redshift of 0.936. The redshift of the lens galaxy was confirmed through 21 cm HI absorption by Carilli et al. (1993). Cohen et al. (2003) obtained a high quality spectrum which confirms the absorption features and clearly detect a strong broad emission line at 5470 Å that identified as Mg II 2800 Å yields a redshift of  $z = 0.944$  for the blazar. In addition these authors claimed the detection of emission lines of [OII],  $H_\beta$  and [OIII] at  $z = 0.684$  attributed to the lens galaxy. Moreover they claimed the detection of weak  $H_\beta$  and [OIII] emission in the red noisy spectrum, also attributed to the blazar at  $z = 0.944$

We obtain an optical spectrum ranging from 4500 to 10000 Å with a SNR in the range 25-50. We confirm the detection of Mg II and Ca II absorption lines at  $z = 0.684$ , and in addition we clearly detect an absorption line at 9920 Å identified as Na I 5892 Å at the redshift of the lens. We do not detect the emissions line [OII],  $H_\beta$  and [OIII] (claimed by Cohen et al. 2003). We note that some of these latter features occur inside the telluric absorptions of the  $O_2$  and  $H_2O$ . We clearly detect the strong broad emission line at 5480 Å (EW=35 Å, FWHM=4700 km/s) that if attributed to Mg II 2800Å, yields the redshift of  $z = 0.954$ . We stress that in our spectrum we do not detect the claimed emissions  $H_\beta$  and [OIII] attributed to the blazar by Cohen et al. (2003). We note again that these features are placed in a spectral region that is heavily contaminated by strong  $H_2O$  atmospheric absorption. Therefore we conclude that the redshift of the S3 0218+357 is still tentative since it is based on only one line. If confirmed, this source is the most distant blazar detected at frequencies  $> 100$  GeV (Ahnen et al. 2016).



It is worth to note that the shape of the continuum exhibits a marked decline towards the blue region that is rather unusual for this type of source. This could be due to significant intrinsic extinction or caused by absorption in the lens.

**3C 66A:** [Wills & Wills \(1974\)](#) identified this strong radio source as a BLL because of its featureless optical spectrum. [Miller et al. \(1978\)](#) proposed a redshift of  $z = 0.444$ , on the basis on one emission line attributed to Mg II 2800 Å. A value considered by the authors as tentative and highly uncertain. No other optical spectroscopy was done for thirty years. More recently [Finke et al. \(2008\)](#) showed an optical spectrum in the range from 4200 to 8500 Å with no detectable optical features. The featureless spectrum was also confirmed by [Shaw et al. \(2013\)](#).

Our high SNR ( $\sim 200$ ) GTC spectrum is also featureless. Based on our procedure of redshift lower limits estimated by  $EW_{min}$ , due to the relatively bright source we can set only a modest lower limit of  $z > 0.10$ . We are not able to confirm the Mg II emission proposed by [Miller et al. \(1978\)](#) because it is out of our spectral range. However at  $z = 0.444$  we would expect to observe  $H_\beta$  emission line at 7020 Å, where we do not detect any line with  $EW > 0.2\text{Å}$ . We conclude that the redshift of this source is still unknown.

**VER J0521+211:** On the basis on a weak emission line at 5940Å attributed to [N II] 6583Å, [Shaw et al. \(2013\)](#) proposed this source to be at  $z = 0.108$ . This feature was not confirmed by [Archambault et al. \(2013\)](#) that reports a featureless spectrum.

We do not confirm the redshift of the source, which therefore is still unknown, setting a lower limit of  $z > 0.18$ .

**1ES 0647+250:** An optical spectrum of this source, with modest SNR was found featureless by [Schachter et al. \(1993\)](#), a result later confirmed by a better spectrum obtained with the Keck telescope by [Shaw et al. \(2013\)](#). A relatively high redshift can be supported by the absence of detection of the host galaxy from high quality image by [Kotilainen et al. \(2011\)](#).

Our GTC higher SNR ( $\sim 200$ ) spectrum confirms this featureless behaviour with absorptions at around 4400 Å and 4880 Å due to Diffusing Interstellar bands (DIBs) and at  $\sim 6500$  Å due to water vapor. On the basis of our spectrum we set a lower limit of  $z > 0.29$ .

**S5 0716+714:** This is a bright ( $V \sim 15$ ) and highly variable ([Bach et al. 2007](#)) source for which several attempts to detect the redshift failed (([Stickel & Kuhr 1993](#); [Rector & Stocke 2001](#); [Finke et al. 2008](#); [Shaw et al. 2013](#))). From optical images [Sbarufatti et al. \(2005a\)](#) set a lower limit of  $z > 0.5$  and [Nilsson et al. \(2008\)](#) provided an imaging redshift of  $z \sim 0.3$  based on the marginal detection of the host galaxy. Finally we note that [Danforth et al. \(2013\)](#), based on the distribution of the absorption systems, set a statistical upper limit  $z \lesssim 0.3$ .

We obtained a featureless optical spectrum during a high state of the source ( $r = 13.6$ ) and we can set a redshift lower limit of  $z > 0.10$ .

**BZB J0915+2933:** [Wills & Wills \(1976\)](#) showed a continuous optical spectrum for the source and classified it as a BLL. The featureless behaviour was also found by [White et al. \(2000\)](#) and by [Shaw et al. \(2013\)](#).

Through our high SNR optical spectrum, we confirm the featureless spectrum and set a lower limit to the redshift of  $z > 0.13$ .

**BZB J1120+4212:** This object (also known as RBS 0970) is a point-like radio source detected by various X-ray surveys (see e.g. [Giommi et al. 2005](#)). Optical spectral classification of the source as BLL was proposed by [Perlman et al. \(1996\)](#) on the basis of the quasi-featureless spectrum. They claim the detection of starlight absorption features at  $z = 0.124$ . However, based on the spectrum reproduced in their Fig. 4, the reliability of this features is quite uncertain. This redshift is not confirmed in other spectra obtained by [White et al. \(2000\)](#) and [Massaro et al. \(2014\)](#). Also the spectrum obtained by SDSS (J112048.06+421212.4) appears to us featureless.

Our spectrum with SNR  $\sim 100$ -190 is featureless and we set a lower limit of  $z > 0.28$ .

**1ES 1215+303:** [Bade et al. \(1998\)](#) reported a redshift  $z = 0.130$  for this target, but no information about the detected lines are given. On the contrary [White et al. \(2000\)](#) showed an optical spectrum claiming a redshift of 0.237, although it appears featureless from their figure.

A more recent spectrum (SNR = 60) obtained by [Ricci et al. \(2015\)](#) was also found featureless. The target was clearly resolved in HST exposures (([Scarpa et al. 2000](#))) revealing a massive elliptical host galaxy, suggesting the source is at low redshift.

Given these different redshift values, we secured a high quality optical spectrum (SNR  $\sim 300$ ) in which we detect two emission lines: [OII] 3727 Å, [OIII] 5007 Å at  $z = 0.131$  (see also Table 5) confirming the low redshift previously reported.

**W Comae:** Weistrop et al. (1985) provided an optical spectrum and estimated a redshift of  $z = 0.102$  based on the detection of [OIII] 5007Å and  $H_\alpha$  emission lines. This redshift was not confirmed by Finke et al. (2008), though their spectra cover only the range from 3800 to 5000 Å. In addition the spectrum obtained by the SDSS (J122131.69+281358.4) proposes a redshift of  $z = 1.26$ . In 2003 the host galaxy of W Comae was resolved by Nilsson et al. (2003).

From our (SNR $\sim 220$ ) optical spectrum we confirm the detection of [O III] 5007Å and  $H_\alpha$  emission lines at  $z = 0.102$ . In addition we detect at the same redshift the absorption lines due to Ca II (3934, 3968 Å) doublet, G-band 4305 Å, and Mg I 5175 Å from the host galaxy.

**MS 1221.8+2452:** A tentative redshift of  $z = 0.218$  was proposed by Morris et al. (1991) and Rector et al. (2000). Imaging studies of this source were able to resolve the host galaxy and are consistent with the low redshift of the target (Falomo & Kotilainen 1999; Scarpa et al. 2000).

We detect the Ca II doublet and G-band 4305 Å absorption lines at  $z=0.218$  and we find emission lines at  $\sim 7995$  and  $\sim 8020$  Å that if confirmed could be attributed to  $H_\alpha$  and N II 6583 Å.

**S3 1227+255:** Nass et al. (1996) reported  $z = 0.135$  but no information on the detected spectral lines were provided. In spite of the alleged low redshift, high quality images failed to detect the host galaxy Nilsson et al. (2003). Shaw et al. (2013) did not confirm this redshift and no spectral features were found.

Our optical spectrum (SNR  $\sim 250$ ) is featureless down to  $EW = 0.1-0.2$  Å. Therefore we do not confirm the literature redshift and we set a redshift lower limit of  $z > 0.10$ .

**BZB J1243+3627:** White et al. (2000) reported a featureless spectrum for this source. An absorption feature of Mg II 2800Å at  $\lambda \sim 4160$  Å was detected in the SDSS spectrum suggesting a redshift of  $z \geq 0.485$  Plotkin et al. (2010). This redshift limit appears consistent with the marginal detection of the host galaxy by Meisner & Romani (2010) who estimated  $z \sim 0.50$ .

From our spectrum (SNR  $\sim 330$ ), we confirm the intervening absorption system due to Mg II 2800Å and the remaining part of the spectrum is completely featureless. The spectroscopic redshift lower limit is thus  $z > 0.483$ .

**BZB J1248+5820:** The source was classified as a BLL by Fleming et al. (1993) and no redshift was available. The featureless nature of the spectrum is reported in (Henstock et al. 1997; Plotkin et al. 2008) and Shaw et al. (2013). Note that NED report  $z = 0.847$  based on the SDSS DR3 spectrum, although this is not confirmed by SDSS DR13 analysis. Scarpa et al. (2000) failed to detect the host galaxy from HST images.

Our high SNR spectrum is featureless and we can determine a lower limit to the redshift of  $z > 0.14$ .

**PKS 1424+240:** The source was classified as BLL by Fleming et al. (1993) and a featureless spectra was reported by Marcha et al. (1996); White et al. (2000) and Shaw et al. (2013). Furniss et al. (2013), from the  $Ly_\beta$  and  $Ly_\gamma$  absorptions observed in the far-UV spectra from HST/COS (Hubble Space Telescope/Cosmic Origins Spectrograph) spectra, reported a lower limit  $z > 0.6035$ . This is consistent with the non detection of the host galaxy in HST images Scarpa et al. (2000).

In our high SNR  $\sim 350$  optical spectrum, we detect two faint emission lines at 5981 and 8034 Å (see Fig.5) due to [O II] 3727Å and [O III] 5007Å. The redshift corresponding to this identification is 0.6047, suggesting that the absorber at that redshift limit is associated to the BLL. Note also that in the environment of the target there is a group of galaxies at  $z \sim 0.60$  suggesting it is associated to the BLL (Rovero et al. 2016).

**BZB J1540+8155:** The source was identified as BLL by Schachter et al. (1993). The optical spectra obtained by Perlman et al. (1996) failed to detect emission or absorption features. The host galaxy was not detected by HST images (Scarpa et al. 2000) posing the source at relatively high redshift.

In our GTC spectrum we detect an intervening absorption doublet at  $\sim 4680$  Å that we identify as MgII 2800 Å absorption yielding a spectroscopic redshift lower limit of  $z > 0.673$ . No intrinsic emission or absorption lines are found. The spectroscopic redshift limit is consistent with our redshift limits determined by the absence of detection of host galaxy features.

**RGB J2243+203:** Laurent-Muehleisen et al. (1998) presents the first optical spectrum of this source, found featureless. Similarly the spectrum obtained by Shaw et al. (2013) is featureless but the authors claimed the detection of an absorption line at  $\sim 3900 \text{ \AA}$  identified as Mg II (2800 $\text{\AA}$ ). If confirmed this would imply a redshift  $z > 0.395$ .

Our spectrum, that does not cover the 3900 $\text{\AA}$  region, is very featureless from 4100 $\text{\AA}$  to 9000 $\text{\AA}$  with the limits on the emission or absorption lines of  $EW_{min} < 0.2$ . This corresponds to a lower limit of  $z > 0.22$ .

**BZB J2323+4210:** From a poor optical spectrum Perlman et al. (1996) claimed the detection of two starlight absorption features identified as Mg I (5175 $\text{\AA}$ ) and Na I (5892  $\text{\AA}$ ) and they proposed at redshift  $z = 0.059$ . We disprove this redshift because the Na I absorption coincides with the telluric absorption at 6280  $\text{\AA}$ . Shaw et al. (2013) does not confirm the above redshift either.

Our high SNR ( $\sim 200$ ) spectrum is characterized by a power law emission ( $F_\lambda \propto \lambda^\alpha$ ;  $\alpha = -1.2$ ). We clearly detect an absorption doublet at  $\sim 5000 \text{ \AA}$  ( $EW \sim 0.25 \text{ \AA}$ ) and an absorption line at 7465  $\text{\AA}$ . We identify these features as Ca II 3934, 3968  $\text{\AA}$ , and Na I 5892 $\text{\AA}$  absorption lines at  $z = 0.267$ . If these lines were ascribed to the starlight of the host galaxy we would expect to observe some modulation imprinted on the continuum, which are not present. Moreover this redshift appears remarkable inconsistent with the lower limits ( $z_{lim} > 0.65$ ) derived from the non detection of the host galaxy.

We further note these absorption features are rather narrow ( $FWHM \sim 10 \text{ \AA}$ ) compared to typical Ca II line width from galaxies and are indicative of interstellar absorptions. Indeed at  $\sim 8.5$  and 12 " (SE) from the target (see Fig.3) there are two spiral galaxies with halo gas which could be responsible of the absorption features observed. At  $z = 0.267$  the projected separation between the target and these galaxies is  $\sim 40 \text{ kpc}$ .

We conclude that the redshift of BZB J2323+4210 is still unknown and we set a spectroscopic lower limit of  $z > 0.267$  and a lower limit based on the host galaxy feature of  $z > 0.65$ .

The case has some analogy with that of the BLL MH 2136-428 (Landoni et al. 2014), where narrow absorption lines appear in the spectrum due to the halo of an interloping bright galaxy.

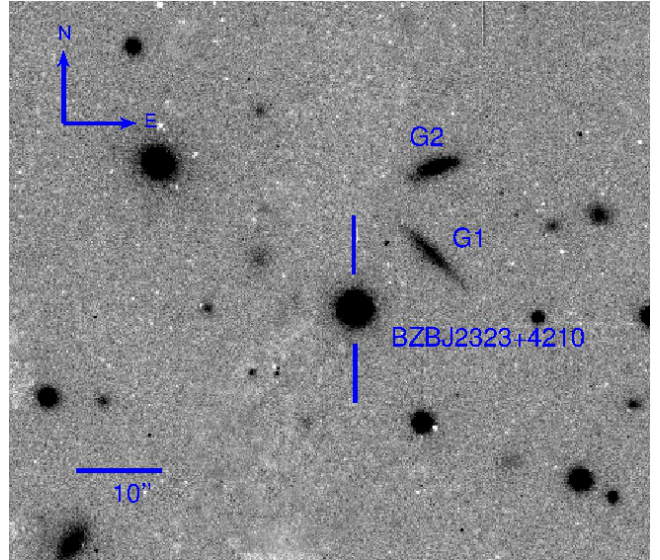


**Figure 3.** Optical R-image of the BL Lac object BZB J2323+4210 taken at the NOT telescope (Falomo & Kotilainen 1999). Two spiral galaxies, labelled as G1 and G2, are present in the field of view of the BL Lac object at a distance of  $\sim 8.5''$  and  $\sim 12.0''$  respectively.

## 6. DISCUSSION

We secured high SNR spectra in the range 4200-9500  $\text{\AA}$  for a sample of 22 BLLs, selected for being TeV emitters or good candidates based on their IR properties. Most of these sources either had unknown redshift or the value was rather uncertain. From the new spectroscopy we are able to determine the redshift for 5 objects (S3 0218+357, 1ES 1215+303, W Comae, MS 1221.8+2452, and PKS 1424+240). For PKS 1424+240, one of the farthest BLL detected in the TeV regime, no previous estimate of the redshift was available. For three objects, BZB J1243+3627 with an uncertain redshift and BZB J1540+8155, and BZB J2323+4210 with previously unknown redshift, we found intervening absorptions that allow us to set spectroscopic lower limits. For the remaining 13 sources we found that in spite of the high SNR their spectrum is featureless. We can set limits to any emission or absorption features to 0.05-0.50  $\text{\AA}$  depending on the SNR of the targets and the wavelength region. For seven of these targets there was a previous tentative redshift that we do not confirm from our observations. The main reasons for this difference are: old spectra have poor SNR, wrong source identification, very tentative line identifications and redshift given without information on the detected spectral features (no spectrum shown). It is worth to note that unfortunately these unconfirmed, likely wrong values (also appearing in NED) are often used to derive physical properties of the sources.

On the basis of the assumption that all the objects with pure featureless spectra are hosted by a massive

elliptical galaxy as is the case of most (virtually all) BLLs, we have then determined a lower limit of their redshift from the minimum detectable EW of some absorption lines of the host galaxy (see Appendix for details). Depending on the brightness of the observed nuclei ( $r = 13.6$  to  $19.9$ ) we can set redshift lower limits for these objects from  $z = 0.1$  to  $z = 0.55$  (see Tab. 3).

In addition to the lower limits of the redshift for objects with featureless spectra we can also estimate an average upper limit to the redshift of the sample of observed targets based on the number of Mg II 2800 Å intervening absorption systems observed in our spectra. Given our observed spectral range we are potentially able to detect Mg II 2800 Å intervening absorption lines (of  $EW \gtrsim 0.2$  Å) for absorbers that are at  $z > 0.5$ . Excluding the objects that are at  $z < 0.5$  (4 sources) we observe 2 absorption systems of Mg II over 18 targets. To evaluate an average upper limit to the redshift of these sources we compute the expected number of Mg II intervening absorptions as a function of the redshift. To this aim we assume the cumulative incidence rates of Mg II absorbers derived for a very extended sample of QSO spectra obtained by SDSS (Zhu & Ménard 2013). It turns out that the average maximum redshift of sample is inferred to be  $z \sim 0.65$ . At higher redshift we would expect to detect many more absorption systems. For instance if the average redshift of these sources were  $z = 1$  we should detect  $\sim 10$  Mg II absorption systems in the spectra of 18 targets.

The relatively low upper limit of the redshift derived above together with the lack of detection of absorption lines from the host galaxies suggests that these targets have a high Nucleus-to-Host galaxy ratio (N/H). For each object with a featureless continuum we have derived a lower limit to the redshift on the basis of the assumption that the source is hosted by a massive early type galaxy (see Appendix for details) and at a given limit of detectable EW of an absorption feature. We can now associate a minimum N/H to these redshift lower limits (see Tab. 3). It turns out that some objects in our sample have a  $N/H > 10$  (assuming the targets are hosted by a standard galaxy (e.g. Falomo et al. 2014). This is significantly higher than the typical value ( $N/H \sim 1$ ) for BLLs for which the host galaxy is directly imaged by HST, and it is similar to that estimated for unresolved sources at relatively high ( $z = 0.5 - 1.0$ ) redshift (see e.g. Urry et al. 2000). Since on average our targets are likely at moderate redshift (see above) the high N/H is suggestive of a particularly beamed nuclear emission. How strong could be the flux from the nucleus compared with that of its host galaxy? For a Doppler factor  $\delta$  extremely high, we could have  $N/H \sim 1000$ . The detection of the spectral features of the host galaxy therefore will require observations with very high SNR

and adequate spectral resolution. This appears feasible only in the ELT era (see e.g. Landoni et al. 2014).



**Table 1.** THE SAMPLE OF TEV BLLAC AND TEV-CANDIDATES

Object name	RA (J2000)	$\delta$ (J2000)	CLASS	V	$E(B - V)$	$z_{literature}$	Reference
BZB J0035+1515	00:35:14.70	15:15:04.0	TeVc	16.9	0.062	?	
1ES 0033+595	00:35:52.60	59:50:05.0	HBL	19.5	1.386	?	
S2 0109+22*	01:12:05.08	22:44:39.0	IBL	15.7	0.034	0.265 ?	<a href="#">Healey et al. (2008)</a>
RGB J0136+391	01:36:32.50	39:06:00.0	HBL	15.8	0.068	?	
S3 0218+357	02:21:05.50	35:56:14.0	HBL**	20.0	0.061	0.944	<a href="#">Cohen et al. (2003)</a>
3C 66A	02:22:39.60	43:02:08.0	IBL	15.0	0.075	0.444 ?	<a href="#">Miller et al. (1978)</a>
VER J0521+211	05:21:45.90	21:12:51.0	IBL	17.5	0.604	0.108 ?	<a href="#">Shaw et al. (2013)</a>
1ES 0647+250	06:50:46.50	25:03:00.0	HBL	15.7	0.087	?	
S5 0716+714	07:21:53.40	71:20:36.0	IBL	15.5	0.027	?	
BZB J0915+2933	09:15:52.40	29:33:24.0	TeVc	15.8	0.021	?	
S4 0954+65***	09:58:47.20	65:33:55.0	LBL	17.0	0.106	0.367 ?	<a href="#">Lawrence et al. (1986)</a>
BZB J1120+4212	11:20:48.00	42:12:12.0	TeVc	17.3	0.001	0.124 ?	<a href="#">Perlman et al. (1996)</a>
1ES 1215+303	12:17:52.10	30:07:01.0	HBL	15.8	0.020	0.13 ?	<a href="#">Bade et al. (1998)</a>
W Comae	12:21:31.70	28:13:59.0	IBL	15.4	0.021	0.102 ?	<a href="#">Weistrop et al. (1985)</a>
MS 1221.8+2452	12:24:24.20	24:36:24.0	HBL	16.7	0.019	0.218 ?	<a href="#">Morris et al. (1991)</a>
S3 1227+255	12:30:14.10	25:18:07.0	IBL	14.7	0.017	0.135 ?	<a href="#">Nass et al. (1996)</a>
BZB J1243+3627	12:43:12.70	36:27:44.0	TeVc	16.2	0.010	?	
BZB J1248+5820	12:48:18.80	58:20:29.0	TeVc	15.4	0.011	?	
PKS 1424+240	14:27:00.40	23:48:00.0	HBL	14.6	0.050	?	
BZB J1540+8155	15:40:15.80	81:55:06.0	TeVc	17.6	0.044	?	
RGB J2243+203	22:43:54.70	20:21:04.0	HBL	16.0	0.042	?	
BZB J2323+4210	23:23:52.10	42:10:59.0	TeVc	17.0	0.134	0.059 ?	<a href="#">Perlman et al. (1996)</a>

Col. 1: Name of the target; Col. 2: Right Ascension; Col. 3: Declination; Col. 4: Class of the source: High-synchrotron peaked BL Lac (HBL), Intermediate-synchrotron peaked BL Lac (IBL), Low-synchrotron peaked BL Lac (LBL), TeV Candidate BL Lac (TeVc); Col. 5: V-band magnitudes taken from NED; Col. 6:  $E(B - V)$  taken from the NASA/IPAC Infrared Science Archive (<https://irsa.ipac.caltech.edu/applications/DUST/>); Col. 7: Redshift; Col. 8: Reference to the redshift.

\* Details for S2 0109+22 are reported in [Paiano et al. \(2016\)](#), \*\* Gravitationally lensed system , \*\*\* = Details for S4 0954+65 are reported in [Landoni et al. \(2015\)](#)

**Table 2.** LOG OBSERVATIONS OF TEV SOURCES AND TEV-CANDIDATES OBTAINED AT GTC

Obejct	Grism B			Grism R			
	$t_{Exp}$ (s)	Date	Seeing	$t_{Exp}$ (s)	Date	Seeing	r
BZB J0035+1515	2100	2015 Sept 30	0.6	1800	2015 Oct 01	0.6	17.00
1ES 0033+595	3600	2015 Sept 18	1.3	2700	2015 Sept 25	0.9	17.80
S2 0109+22	750	2015 Sept 19	1.8	750	2015 Sept 19	1.8	15.20
RGB J0136+391	900	2015 Sept 28	0.9	600	2015 Sept 28	0.9	15.80
S3 0218+357	3600	2015 Feb 05	0.9	8700	2015 Feb 05	1.2	19.90
3C 66A	750	2015 Sept 09	0.8	210	2015 Sept 06	0.8	14.70
VER J0521+211	900	2015 Sept 21	0.8	1050	2015 Sept 21	0.8	16.40
1ES 0647+250	1500	2015 Sept 22	1.4	1200	2015 Sept 22	1.4	15.80
S5 0716+714	210	2015 Nov 30	1.6	210	2015 Nov 30	1.6	13.60
BZB J0915+2933	750	2015 Dec 24	2.0	450	2015 Jun 06	2.0	15.90
S4 J0954+65	300	2015 Feb 28	1.0	450	2015 Feb 28	1.0	15.5
BZB J1120+4212	3000	2016 Jun 24	1.5	3600	2015 Jul 01	0.7	16.10
1ES 1215+303	900	2015 May 20	1.5	900	2015 May 20	1.5	14.50
W Comae	1800	2015 Jun 30	1.4	1800	2015 Jun 30	1.4	15.50
MS 1221.8+2452	3000	2015 May 31	1.3	3000	2015 May 31	1.2	16.70
S3 1227+255	450	2015 Dec 25	1.5	500	2015 Dec 25	1.5	14.90
BZB J1243+3627	1350	2015 May 21	1.2	1350	2015 May 21	1.2	15.60
BZB J1248+5820	600	2015 Dec 25	2.2	900	2015 Dec 25	2.2	15.70
PKS 1424+240	450	2015 Jun 30	1.0	450	2015 Jun 30	1.0	14.20
BZB J1540+8155	900	2015 Jun 23	1.0	900	2015 Jun 23	1.0	17.30
RGB J2243+203	600	2015 Sept 19	2.0	750	2015 Sept 19	2.0	16.20
BZB J2323+4210	3000	2016 Aug 07	1.3	3600	2015 Feb 28	0.7	17.50

Col.1: Name of the target; Col.2: Total integration time with the Grism B; Col.3: Date of Observation with Grism B; Col.4: Seeing during the observation with the Grism B; Col.5: Total integration time with the Grism R; Col.6: Date of Observation with Grism R; Col.7: Seeing during the observation with the Grism R; Col.8: r' mag measured on the acquisition images.

**Table 3.** PROPERTIES OF THE OPTICAL SPECTRA OF OBSERVED SOURCES

OBJECT	$\alpha$	SNR	$EW_{min}$	$z_{lim}$	$z$	$N/H_{lim}$
BZB J0035+1515	-1.3	183-275	0.09-0.18	0.55 (0.32)		11
1ES 0033+595	*	40-135	0.27-0.52	0.53 (0.10)	0.467 <sup>e</sup>	5
S2 0109+22	-1.0	167-375	0.07-0.16	0.35 (0.15)		20
RGB J0136+391	-1.5	196-482	0.08-0.15	0.27 (0.14)		6
S3 0218+357	*	5-20	*	*	0.944 <sup>e</sup>	3
3C 66A	-1.1	118-314	0.10-0.22	0.10 (*)		2
VER J0521+211	-0.9	82-221	0.15-0.37	0.18 (0.10)		1
1ES 0647+250	-1.3	115-294	0.09-0.21	0.29 (0.12)		7
S5 0716+714	-0.8	180-346	0.04-0.14	0.10 (*)		4
BZB J0915+2933	-1.1	89-241	0.14-0.34	0.13 (*)		1
S4 J0954+65	-0.9	50-120	0.15-0.20	0.45 (0.27)		25
BZB J1120+4212	-1.6	100-190	0.12-0.23	0.28 (0.12)		5
1ES 1215+303	-1.0	205-375	0.09-0.14	0.14 (*)	0.129 <sup>e</sup>	4
W Comae	-0.6	180-260	0.09-0.17	0.19 (0.10)	0.102 <sup>e,g</sup>	1
MS 1221.8+2452	-1.2	115-199	0.13-0.23	0.34 (0.15)	0.218 <sup>e,g</sup>	2
S3 1227+25	-0.8	124-397	0.09-0.24	0.10 (*)		2
BZB J1243+3627	-1.3	208-465	0.05-0.15	0.28 (0.10)	>0.48 <sup>a</sup>	29
BZB J1248+5820	-0.9	76-225	0.12-0.29	0.14 (*)		2
PKS 1424+240	-1.1	254-436	0.04-0.10	0.10 (*)	0.604 <sup>e</sup>	184
BZB J1540+8155	-1.3	97-211	0.15-0.28	0.56 (0.22)	>0.67 <sup>a</sup>	14
RGB J2243+203	-1.1	109-178	0.15-0.22	0.22 (0.10)		3
BZB J2323+4210	-1.2	160-315	0.07-0.17	0.73 (0.65)	>0.267 <sup>a</sup>	1

Col.1: Name of the target; Col.2: Optical spectral index derived from a Power Law fit in the range 4250-10000; Col.3: range of SNR of the spectrum; Col.4: Range of the minimum equivalent width ( $EW_{min}$ ) derived from different regions of the spectrum (see text), Col.5: Lower limit ( $3\sigma$  level) of the redshift by assuming BL Lac host galaxy with  $M_R = -22.9$  (-21.9), in parenthesis we give the redshift lower limit assuming a host galaxy one magnitude fainter. An asterisk indicates that the redshift limit is out of observed range for the case of fainter host galaxy (see Appendix), Col.6: Spectroscopic redshift; the superscript letters are: *e* = emission line, *g* = host galaxy absorption, *a*= intervening absorption ; Col.7: Lower limit of the Nucleus-Host galaxy Ratio (N/H) in r-band considering the whole flux of the host galaxy.

**Table 4.** CORRESPONDENCE BETWEEN THE WAVELENGTH RANGE, ABSORPTION LINES AND REDSHIFT RANGE

Wavelength Range	Absorption Line	Redshift Range
4250 - 5000	CaII	0.08 - 0.27
5000 - 6200	CaII	0.27 - 0.58
6400 - 6800	CaII	0.63 - 0.73
7800 - 8100	MgI	0.51 - 0.57
8400 - 8900	MgI	0.63 - 0.72

Col.1: Wavelength range of the optical spectrum; Col.2: Host galaxy absorption line used; Col.3: Redshift range corresponding to the wavelength range

**Table 5.** MEASUREMENTS OF SPECTRAL LINES

OBJECT	$\lambda_{obs}$ Å	EW (observed) Å	Line ID	$z_{line}$
1ES 0033+595	5468	0.40	[OII] 3727	0.467
S3 0218+357	5470	46.8	Mg II 2800	0.954
1ES 1215+303	4214	0.16	[O II] 3727	0.131
	5661	0.11	[O III] 5007	0.131
W Comae	4747	0.15	G-band 4305	0.102
	5520	0.65	[O III] 5007	0.102
	5704	0.30	Mg I 5175	0.102
	6496	0.31	Na I 5892	0.102
MS 1221.8+2452	4794	0.18	Ca II 3934	0.218
	4834	0.16	Ca II 3968	0.218
	5244	0.20	G-band 4305	0.218
	7995	0.35	H $_{\alpha}$ 6563	0.218
	8022	0.40	N II 6583	0.218
BZB J1243+3627	4150	0.90	Mg II 2800	>0.483
PKS 1424+240	5981	0.05	[O II] 3727	0.604
	8035	0.10	[O III] 5007	0.604
BZB J1540+8155	4680	0.60	Mg II 2800	>0.672
BZB J2323+4210	4987	0.30	Ca II 3934	>0.267
	5031	0.22	Ca II 3968	>0.267
	7470	0.35	Na I 5892	>0.267

Col. 1: Name of the target; Col. 2: Barycenter of the detected line; Col. 3: Measured equivalent width; Col. 4: Line identification; Col. 5: Spectroscopic redshift.



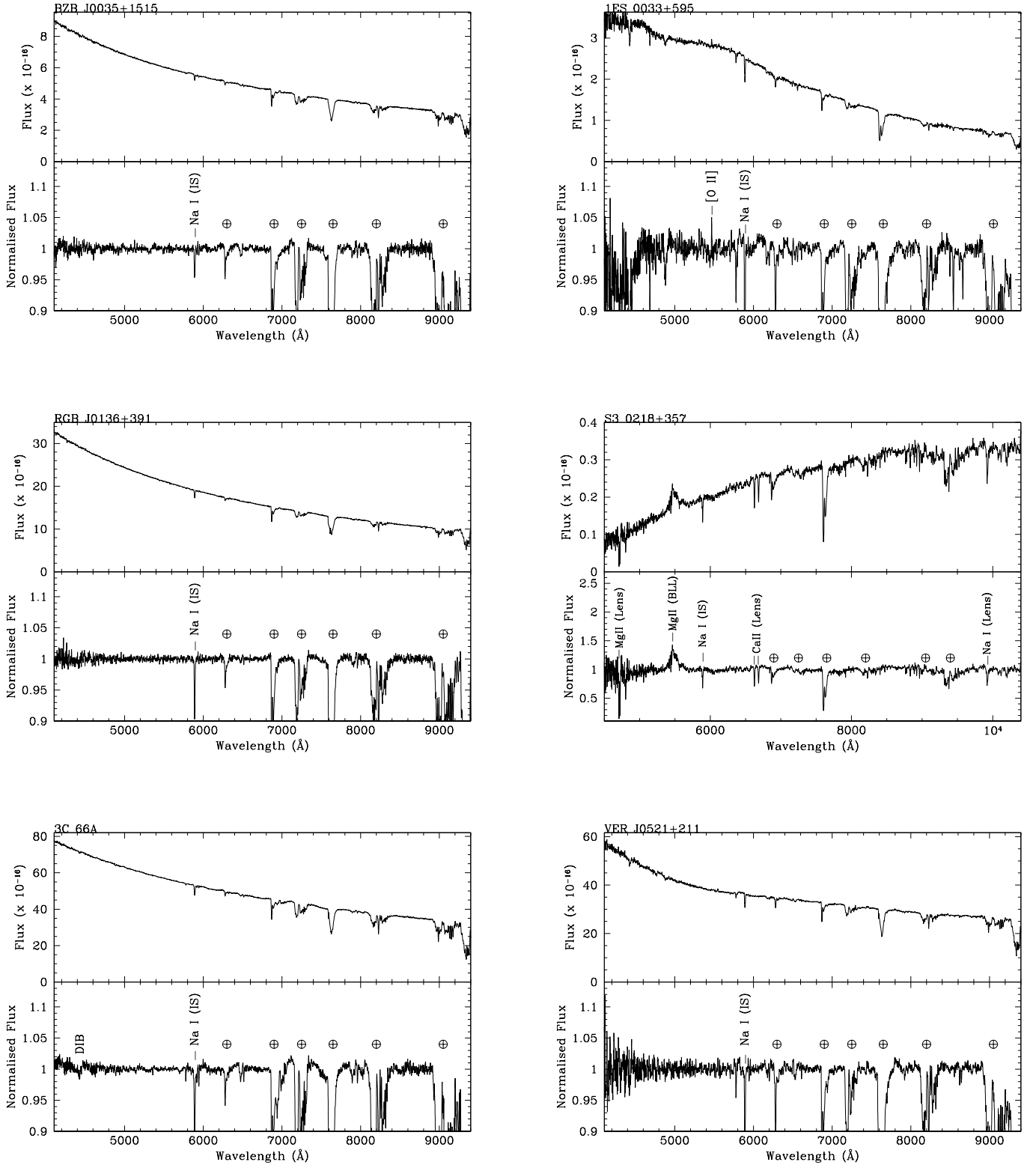


**Figure 4.** Spectra of the TeV sources and TeV-candidates obtained at GTC. *Top panel:* Flux calibrated and dereddered spectra. *Bottom panel:* Normalized spectra. The main telluric bands are indicated by  $\oplus$ , the absorption features from interstellar medium of our galaxies are labelled as IS (Inter-Stellar)

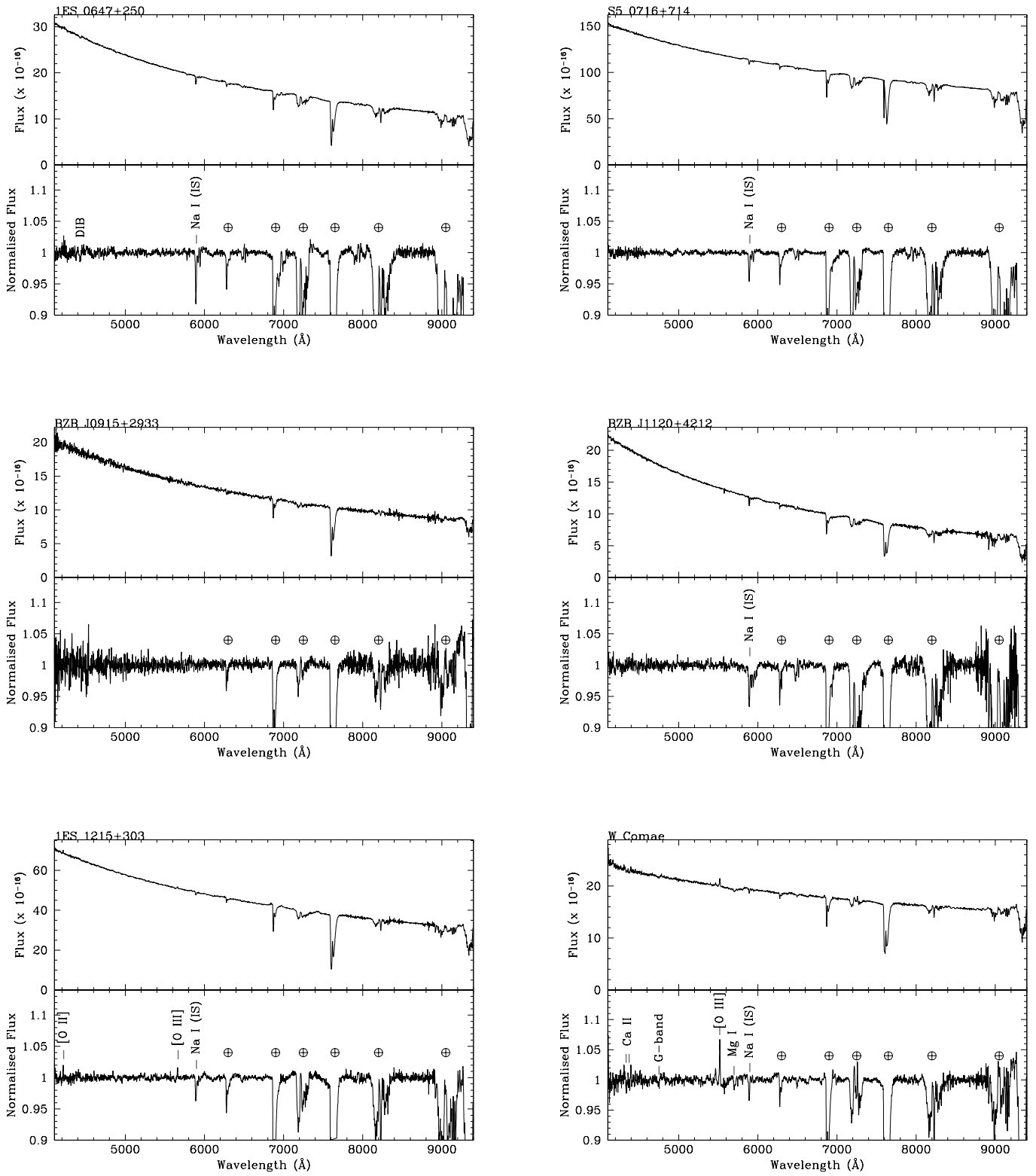


Figure 4. Continued from Fig. 4.

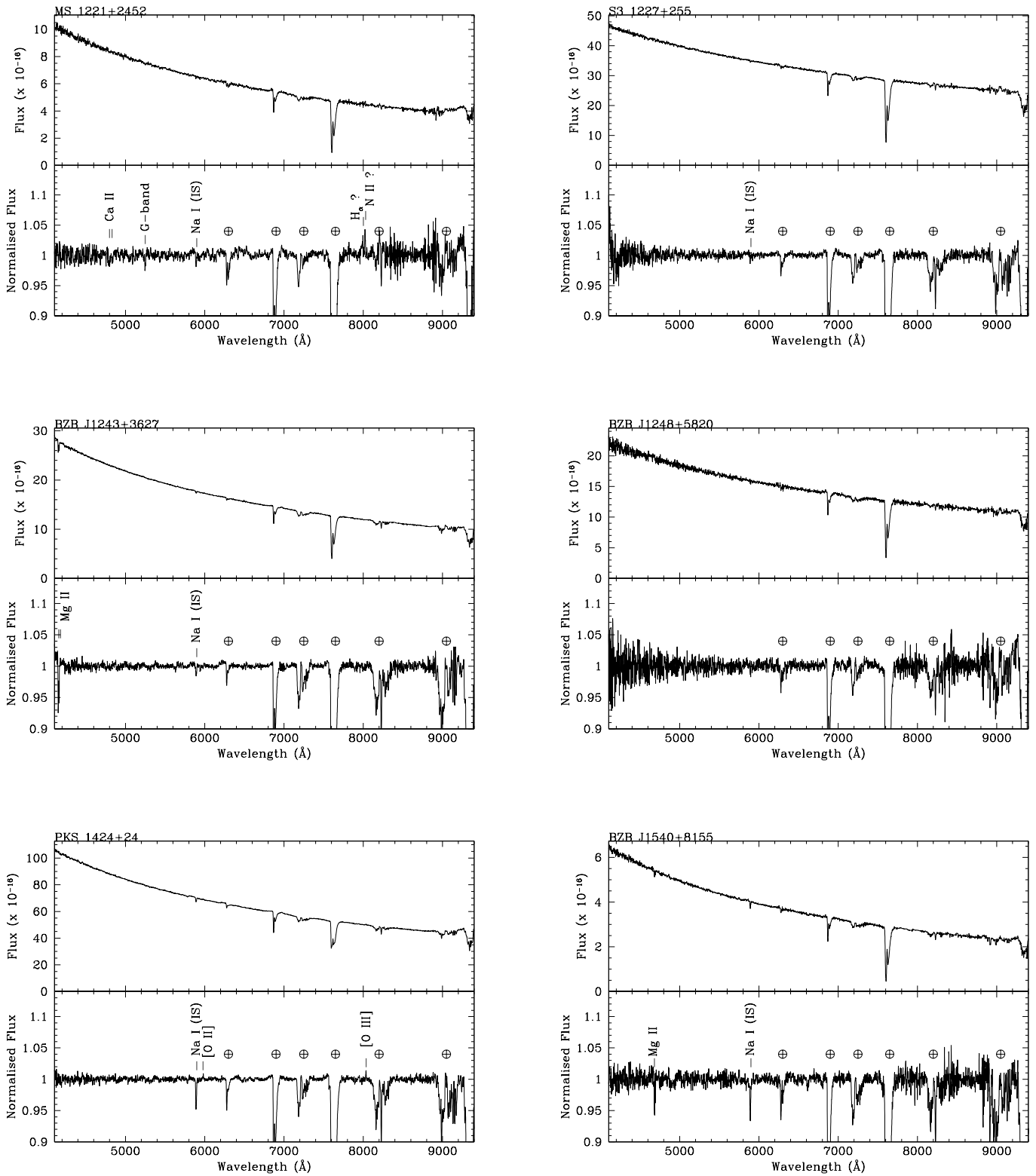


Figure 4. Continued.

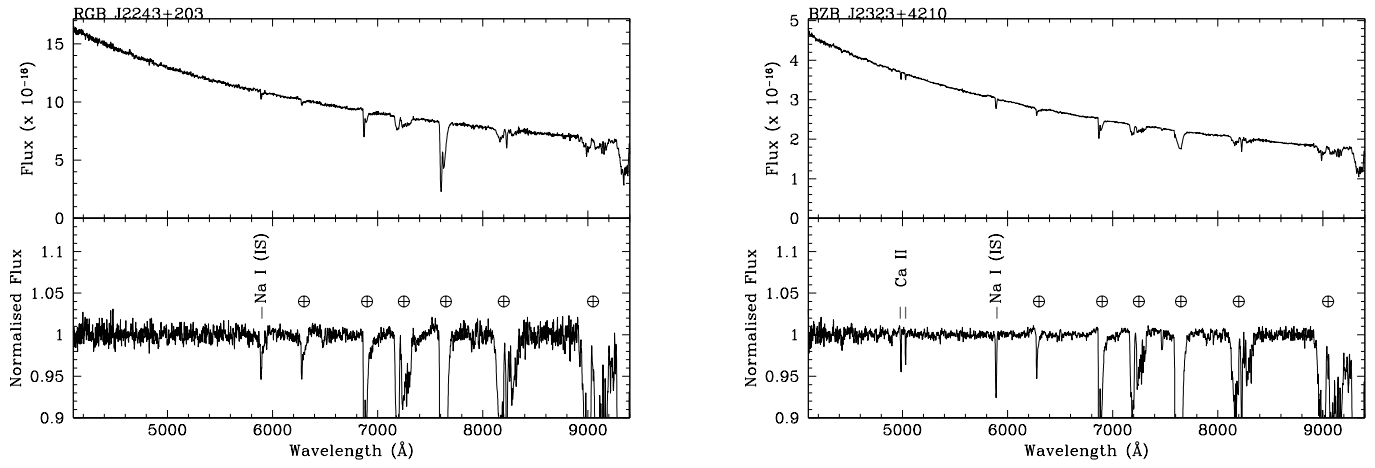
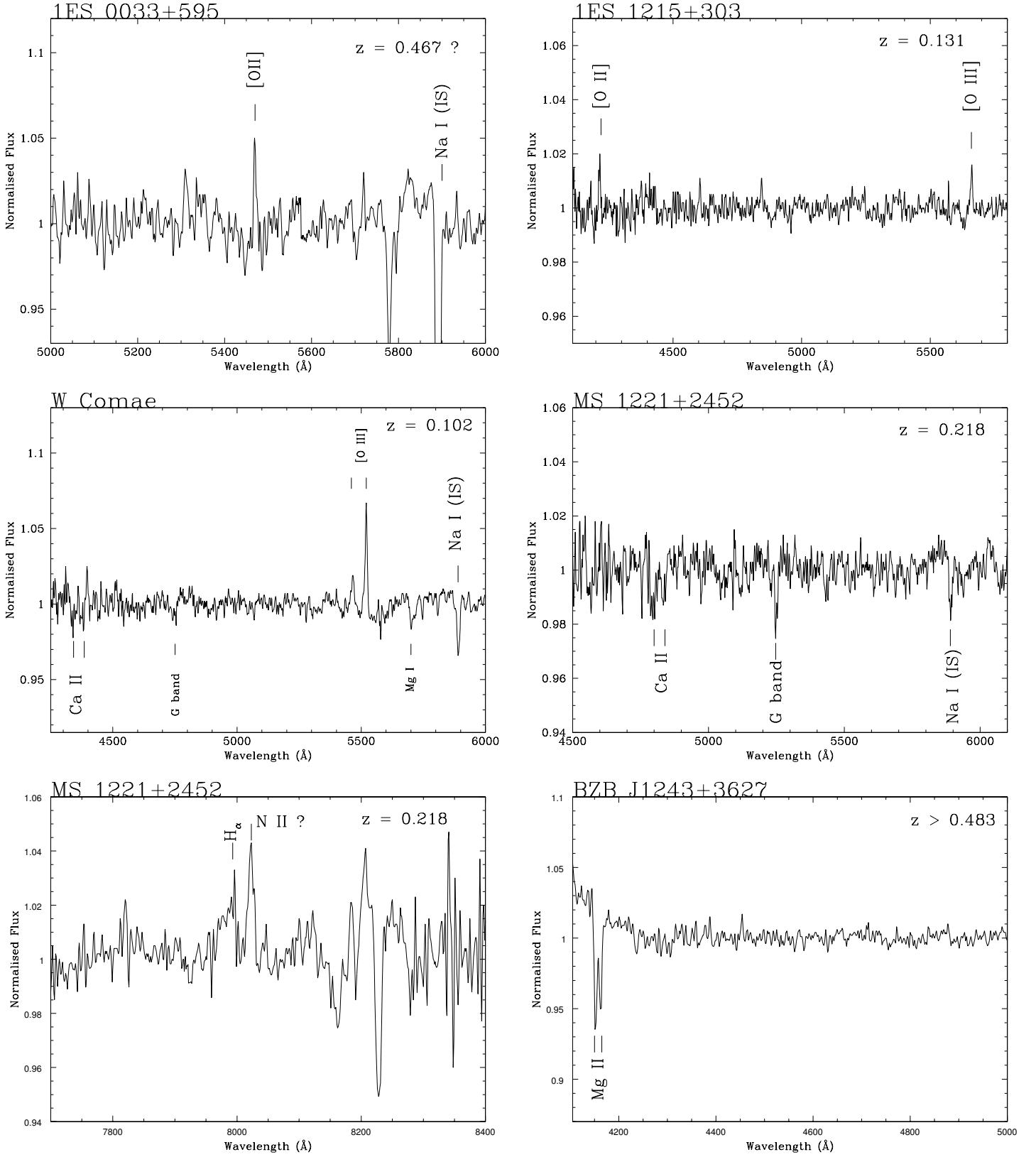


Figure 4. Continued.





**Figure 5.** Close-up of the normalized spectra around the detected spectral features of the TeV sources and TeV-candidates obtained at GTC. Main telluric bands are indicated as  $\oplus$ , spectral lines are marked by line identification.

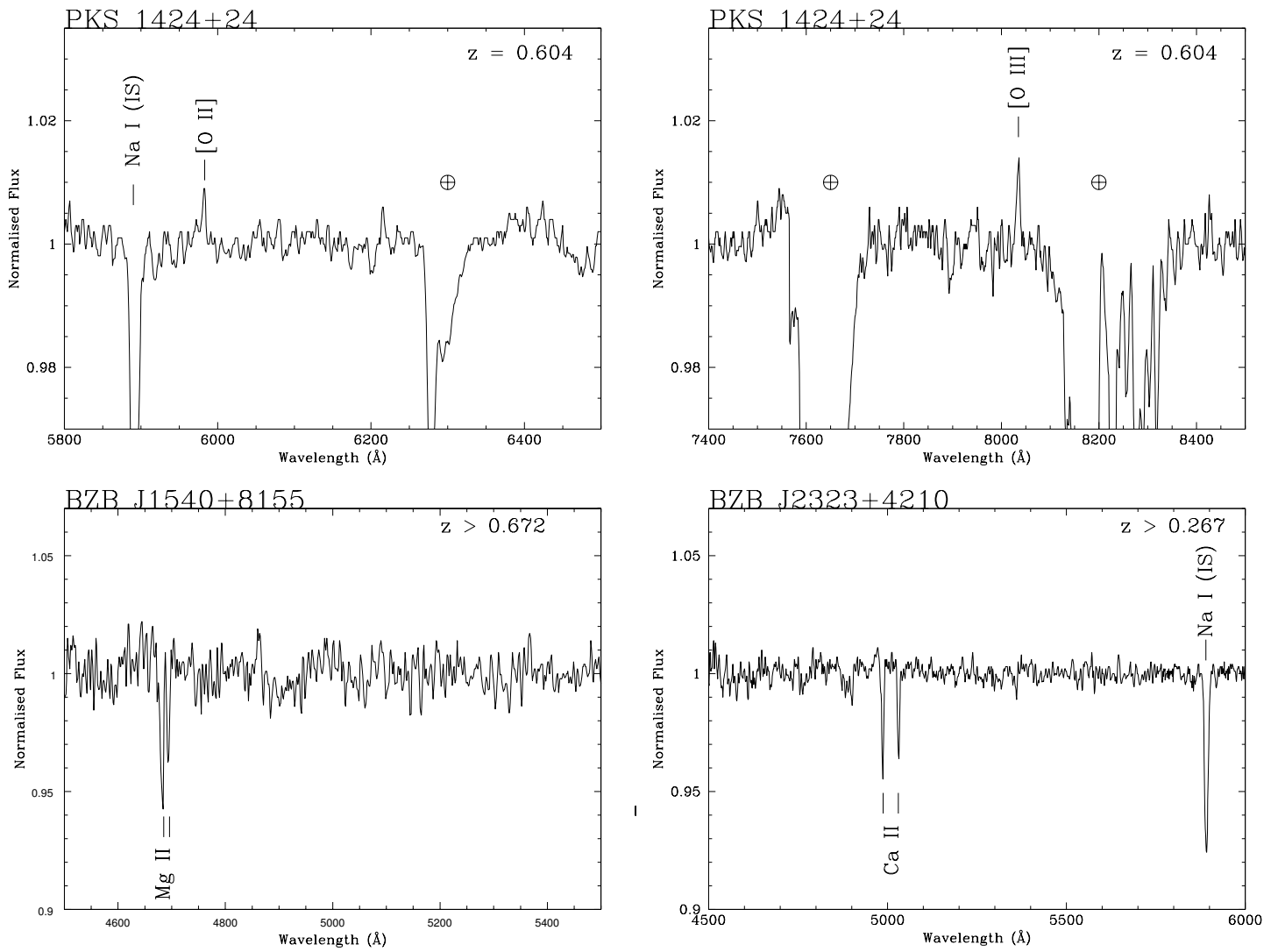


Figure 5. Continued.

## REFERENCES

- Ahnen, Ansoldi, S., Antonelli, L. A., et al. 2016, ArXiv e-prints, arXiv:1609.01095
- Álvarez Crespo, N., Masetti, N., Ricci, F., et al. 2016, *AJ*, 151, 32
- Archambault, S., Arlen, T., Aune, T., et al. 2013, *ApJ*, 776, 69
- Bach, U., Raiteri, C. M., Villata, M., et al. 2007, *A&A*, 464, 175
- Bade, N., Beckmann, V., Douglas, N. G., et al. 1998, *A&A*, 334, 459
- Browne, I. W. A., Patnaik, A. R., Walsh, D., & Wilkinson, P. N. 1993, *MNRAS*, 263, L32
- Cardelli, J. A., Clayton, G. C., & Mathis, J. S. 1989, *ApJ*, 345, 245
- Carilli, C. L., Rupen, M. P., & Yanny, B. 1993, *ApJL*, 412, L59
- Cepa, J., Aguiar-Gonzalez, M., Bland-Hawthorn, J., et al. 2003, in *Proc. SPIE*, Vol. 4841, -, 1739–1749
- Cohen, J. G., Lawrence, C. R., & Blandford, R. D. 2003, *ApJ*, 583, 67
- Danforth, C. W., Nalewajko, K., France, K., & Keeney, B. A. 2013, *ApJ*, 764, 57
- Falomo, R., & Kotilainen, J. K. 1999, *A&A*, 352, 85
- Falomo, R., Pian, E., & Treves, A. 2014, *A&A Rv*, 22, 73
- Finke, J. D., Shields, J. C., Böttcher, M., & Basu, S. 2008, *A&A*, 477, 513
- Fischer, J.-U., Hasinger, G., Schwobe, A. D., et al. 1998, *Astronomische Nachrichten*, 319, 347
- Fleming, T. A., Green, R. F., Jannuzi, B. T., et al. 1993, *AJ*, 106, 1729
- Furniss, A., Williams, D. A., Danforth, C., et al. 2013, *ApJL*, 768, L31
- Giommi, P., Piranomonte, S., Perri, M., & Padovani, P. 2005, *A&A*, 434, 385
- Healey, S. E., Romani, R. W., Cotter, G., et al. 2008, *ApJS*, 175, 97
- Henstock, D. R., Browne, I. W. A., Wilkinson, P. N., & McMahon, R. G. 1997, *MNRAS*, 290, 380
- Jackson, N., Xanthopoulos, E., & Browne, I. W. A. 2000, *MNRAS*, 311, 389
- Kinney, A. L., Calzetti, D., Bohlin, R. C., et al. 1996, *ApJ*, 467, 38
- Kotilainen, J. K., Hyvönen, T., Falomo, R., Treves, A., & Uslenghi, M. 2011, *A&A*, 534, L2
- Landoni, M., Falomo, R., Treves, A., & Sbarufatti, B. 2014, *A&A*, 570, A126
- Landoni, M., Falomo, R., Treves, A., et al. 2013, *AJ*, 145, 114
- . 2012, *A&A*, 543, A116
- Landoni, M., Falomo, R., Treves, A., Scarpa, R., & Reverte Payá, D. 2015, *AJ*, 150, 181
- Laurent-Muehleisen, S. A., Kollgaard, R. I., Ciardullo, R., et al. 1998, *ApJS*, 118, 127
- Lawrence, C. R., Pearson, T. J., Readhead, A. C. S., & Unwin, S. C. 1986, *AJ*, 91, 494
- Marcha, M. J. M., Browne, I. W. A., Impey, C. D., & Smith, P. S. 1996, *MNRAS*, 281, 425
- Massaro, E., Giommi, P., Leto, C., et al. 2009, *A&A*, 495, 691
- Massaro, F., Landoni, M., D’Abrusco, R., et al. 2015, *A&A*, 575, A124
- Massaro, F., Masetti, N., D’Abrusco, R., Paggi, A., & Funk, S. 2014, *AJ*, 148, 66
- Massaro, F., Paggi, A., Errando, M., et al. 2013, *ApJS*, 207, 16
- Meisner, A. M., & Romani, R. W. 2010, *ApJ*, 712, 14
- Miller, J. S., French, H. B., & Hawley, S. A. 1978, in *BL Lac Objects*, ed. A. M. Wolfe, 176–187
- Morris, S. L., Stocke, J. T., Gioia, I. M., et al. 1991, *ApJ*, 380, 49
- Nass, P., Bade, N., Kollgaard, R. I., et al. 1996, *A&A*, 309, 419
- Nilsson, K., Pursimo, T., Heidt, J., et al. 2003, *A&A*, 400, 95
- Nilsson, K., Pursimo, T., Sillanpää, A., Takalo, L. O., & Lindfors, E. 2008, *A&A*, 487, L29
- Nilsson, K., Pursimo, T., Villforth, C., et al. 2012, *A&A*, 547, A1
- Paiano, S., Landoni, M., Falomo, R., Scarpa, R., & Treves, A. 2016, *MNRAS*, 458, 2836
- Patnaik, A. R., Browne, I. W. A., King, L. J., et al. 1993, *MNRAS*, 261, 435
- Perlman, E. S., Stocke, J. T., Schachter, J. F., et al. 1996, *ApJS*, 104, 251
- Piranomonte, S., Perri, M., Giommi, P., Landt, H., & Padovani, P. 2007, *A&A*, 470, 787
- Plotkin, R. M., Anderson, S. F., Hall, P. B., et al. 2008, *AJ*, 135, 2453
- Plotkin, R. M., Anderson, S. F., Brandt, W. N., et al. 2010, *AJ*, 139, 390
- Rector, T. A., & Stocke, J. T. 2001, *AJ*, 122, 565
- Rector, T. A., Stocke, J. T., Perlman, E. S., Morris, S. L., & Gioia, I. M. 2000, *AJ*, 120, 1626
- Ricci, F., Massaro, F., Landoni, M., et al. 2015, *AJ*, 149, 160
- Rovero, A. C., Muriel, H., Donzelli, C., & Pichel, A. 2016, *A&A*, 589, A92
- Sbarufatti, B., Ciprini, S., Kotilainen, J., et al. 2008, ArXiv e-prints, arXiv:0810.3563
- Sbarufatti, B., Falomo, R., Treves, A., & Kotilainen, J. 2006a, *A&A*, 457, 35
- Sbarufatti, B., Treves, A., & Falomo, R. 2005a, *ApJ*, 635, 173
- Sbarufatti, B., Treves, A., Falomo, R., et al. 2005b, *AJ*, 129, 559
- . 2006b, *AJ*, 132, 1
- Scarpa, R., Urry, C. M., Falomo, R., et al. 1999, *ApJ*, 521, 134
- Scarpa, R., Urry, C. M., Padovani, P., Calzetti, D., & O’Dowd, M. 2000, *ApJ*, 544, 258
- Schachter, J. F., Stocke, J. T., Perlman, E., et al. 1993, *ApJ*, 412, 541
- Shaw, M. S., Romani, R. W., Cotter, G., et al. 2013, *ApJ*, 764, 135
- Stickel, M., & Kuhr, H. 1993, *A&AS*, 101, 521
- Tavecchio, F., Roncadelli, M., & Galanti, G. 2015, *Physics Letters B*, 744, 375
- Urry, C. M., Scarpa, R., O’Dowd, M., et al. 2000, *ApJ*, 532, 816
- van Dokkum, P. G. 2001, *PASP*, 113, 1420
- Wei, J. Y., Xu, D. W., Dong, X. Y., & Hu, J. Y. 1999, *A&AS*, 139, 575
- Weistrop, D., Shaffer, D. B., Hintzen, P., & Romanishin, W. 1985, *ApJ*, 292, 614
- White, R. L., Becker, R. H., Gregg, M. D., et al. 2000, *ApJS*, 126, 133
- Wills, B. J., & Wills, D. 1974, *ApJL*, 190, L97
- Wills, D., & Wills, B. J. 1976, *ApJS*, 31, 143
- York, T., Jackson, N., Browne, I. W. A., Wucknitz, O., & Skelton, J. E. 2005, *MNRAS*, 357, 124
- Zhu, G., & Ménard, B. 2013, *ApJ*, 770, 130

## APPENDIX

A. REDSHIFT LOWER LIMIT OF BL LAC  
OBJECTS FROM HOST GALAXY  
ABSORPTION LINES

Given the featureless nature of many BL Lac sources it is of great interest to estimate lower limits of the redshift

for these kind of targets and in particular for those that are also emitters (or candidates) at  $\gamma$  frequencies. In the cases where no spectral features are detected the only way to estimate the redshift or a lower limit from optical data is to use the characteristics of the host galaxies. A

direct method is to use high quality images to detect the surrounding nebulosity, or to assess upper limits of the host brightness and then derive a redshift lower limit. Alternatively one can search for the host galaxy features that are heavily obscured by the dominant non thermal emission (Sbarufatti et al. 2006a). In the first case high resolution and deep images are required while in the second one very high SNR spectra of adequate resolution are needed. Here we focus on this second approach.

Assuming the observed targets have giant elliptical host galaxies of similar luminosity distribution of the population of BLLs for which the host galaxy has been resolved it is plausible to assume that they are hosted by massive early type galaxies (see e.g. Falomo et al. (2014) and references therein). Since the luminosity distribution of these host galaxies is relatively narrow (see e.g. Urry et al. 2000) it is possible to use the host galaxy luminosity as a sort of standard candle to evaluate the distance of the objects or to set lower limits in the cases where no signature from the starlight is found (Sbarufatti et al. (2006a)).

In order to estimate lower limits to the redshift of line-less objects we follow and extend the procedure proposed by Sbarufatti et al. (2006a) for good SNR optical spectra. The basic idea is that under the assumption that the observed spectrum is due to the contribution of a (often dominant) non thermal component, usually described by a power law, and to starlight component from a *standard* host galaxy (see example Fig. A1), it is possible to set lower limits to their redshift

In fact the effect of the strong non thermal emission is to dilute the equivalent width of the absorption features of the host galaxy depending on the flux ratio of the two components (non thermal and starlight). Using high SNR spectra it is thus possible to set suitable upper limits to the equivalent width of the absorption features from the host galaxy. These limits depend on the SNR and the spectral resolution of the observations and on the brightness of the source.

We assume that the underlying host galaxy is a giant elliptical of absolute magnitude  $M(R) = -22.9$  (Sbarufatti et al. (2005a)) and as spectrum template that of Kinney et al. (1996).

For each observed spectrum we then evaluate the dilution factor of an absorption line (namely H,K of Ca II 3924, 3970 Å, G band 4304 Å, Mg I 5175 Å) of this host galaxy as a function of the redshift. To perform this we took into account both k-correction (using the host galaxy template spectrum) and the starlight flux lost through the slit. The latter term was computed by assuming the host galaxy has a de Vaucouleurs brightness profile and an effective radius  $R_e = 8$  kpc.

From the observed magnitude of the source and the assumption that the underlying host galaxy is a giant ellip-

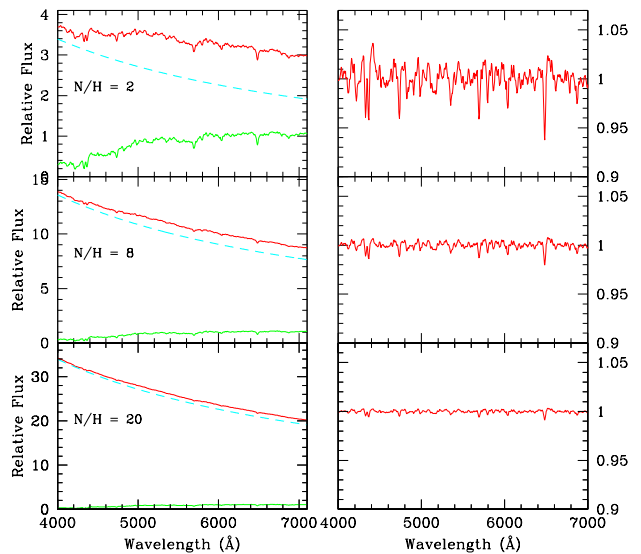


**Figure A1.** LEFT: Simulation of the optical spectrum of a BL Lac object at  $z = 0.2$  for different nucleus to host galaxy ratio ( $N/H$ ). The values of  $N/H$  refer to  $r$  band. The non thermal component is assumed a power law with spectral index  $-1$ . No noise is included. RIGHT: The normalized spectrum of the source (non thermal plus starlight). The figure illustrates the effect of the non thermal component to dilute the equivalent width of the spectral features.

tical we derive the minimum redshift of the target from the minimum detectable equivalent width ( $EW_{min}$ ) of a specific absorption feature (see example in Fig. A3). This depends on the SNR of the spectrum and the brightness of the object during the observations. To estimate  $EW_{min}$  we computed the nominal EW adopting a running window of fixed size (typically 15 Å) for a number of intervals where the SNR is approximately constant and avoiding the prominent telluric absorption bands. For each interval we define  $EW_{min} = 3 \times \sigma_{EW}$  where  $\sigma_{EW}$  is the standard deviation of the distribution of all measurements of EW (see Fig. A2) For each spectral interval a given feature (for instance Ca II absorption) is considered detected only if the SNR is sufficiently high to measure the absorption feature with  $EW > EW_{min}$ . In Figure A4 we show an example of simulated optical spectra of BLLs in the region of Ca II absorption lines assuming different values for the  $N/H$  and SNR.

We used the  $EW_{min}$  of CaII and MgI to derive lower limits to the redshift of featureless BLLs in our sample (see Tab.3 and Tab.4). These limits range from 0.1 to 0.55 Å. For a number of sources other authors have derived redshift limits based on a similar approach but with somewhat different results. In particular Shaw



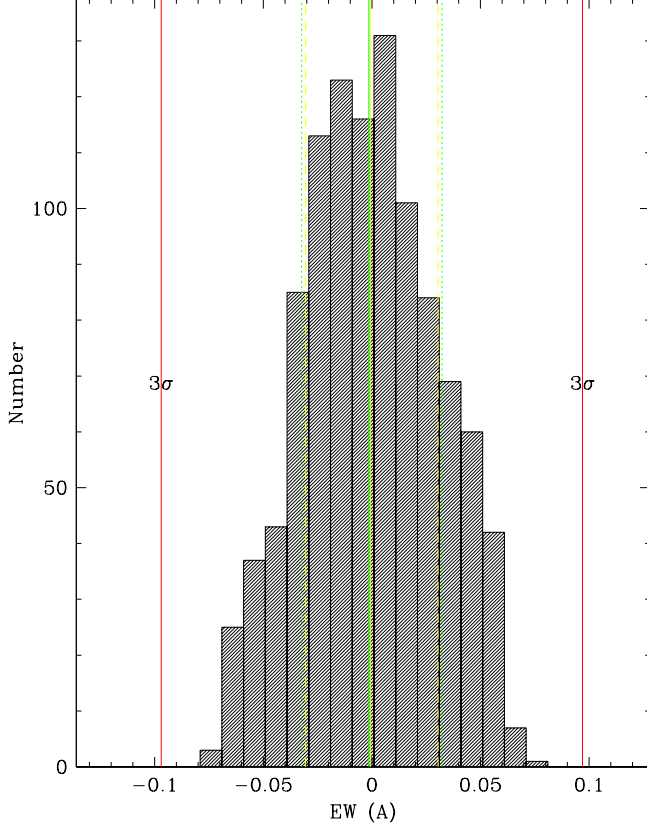


**Figure A2.** Distribution of all measurements of EW computed in a defined spectral interval (avoiding the telluric bands) adopting a running window of fixed size. The  $EW_{min}$  is defined as 3 times  $\sigma_{EW}$  where  $\sigma_{EW}$  is the standard deviation of the distribution (see text for more details).

[et al. \(2013\)](#) propose redshift limits for 15 objects of our sample. For about half of them the difference of redshift limit is small and could be explained by some differences in the adopted method. [Shaw et al. \(2013\)](#) adopt the method proposed by [Plotkin et al. \(2010\)](#) who perform a best fit of the observed spectrum with a host galaxy template and a power law and set a  $2\sigma$  level threshold to assess the redshift (compared with  $3\sigma$  assumed in our work). However, in some cases [Shaw et al. \(2013\)](#) claim redshift limits that are significantly higher than those derived in this work. For instance in the case of RGB J0136+391 we found  $z > 0.27$  while [Shaw](#)

[et al. \(2013\)](#) gives  $z > 0.88$ . The brightness level of the source was similar during the two observations and also the SNR (estimated roughly only from the figures presented by [Shaw et al.](#)) We believe that the latter value is implausible since at this redshift the bluest starlight feature (the CaII absorption lines) should be apparent at  $\lambda > 7450\text{\AA}$ . Since the observed flux at this wavelength is  $\sim 15 \times 10^{-16}$ , the contribution of the host galaxy should be one hundredth of this observed flux. This

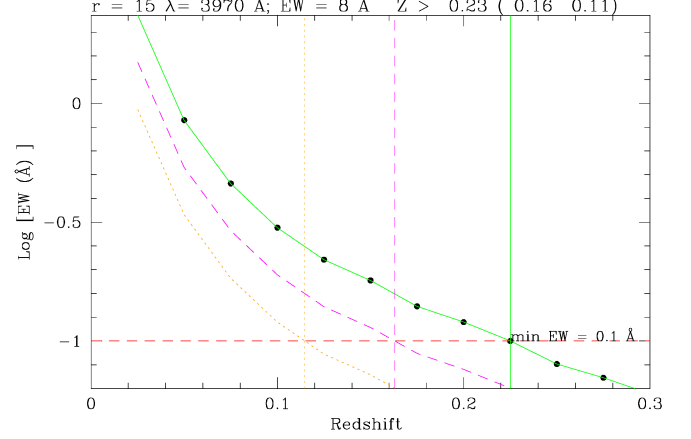


**Figure A3.** The relation between the EW of Ca II absorption feature (assuming  $EW = 8\text{\AA}$ ) and the redshift for the spectrum of a BL Lac object of magnitude  $r = 15$ . The relation assumes that the host galaxy has  $M(R) = -22.9$  (green solid line and filled circles). The other two similar relations are for  $M(R) = -22.4$  (magenta dashed lines) and  $M(R) = -21.9$  (orange dotted line). The dashed horizontal line gives the assumed  $EW_{min}$  level ( $0.1\text{\AA}$ ) and the vertical lines represent the intersection with the above relationships with  $EW_{min}$  level. In this case the redshift is  $z > 0.23$  (for the average host galaxy; other values in parenthesis)

would imply the ability to detect spectral absorption with  $EW \sim 0.01\text{\AA}$  that is inconsistent with the spectral resolution and SNR of the presented data. Another clear discrepant case is that of BZB J0915+2933 for which we give  $z > 0.13$  while [Shaw et al.](#) reports  $z > 0.53$ . In this case the source was a factor  $\sim 5$  fainter, that could help to detect the starlight component, however their SNR is visually worse ( $\sim 30-50$ ) than that of our spectra ( $\sim 100-200$ ) therefore the detection of the host galaxy signature at  $z \sim 0.5$  is very unlikely.

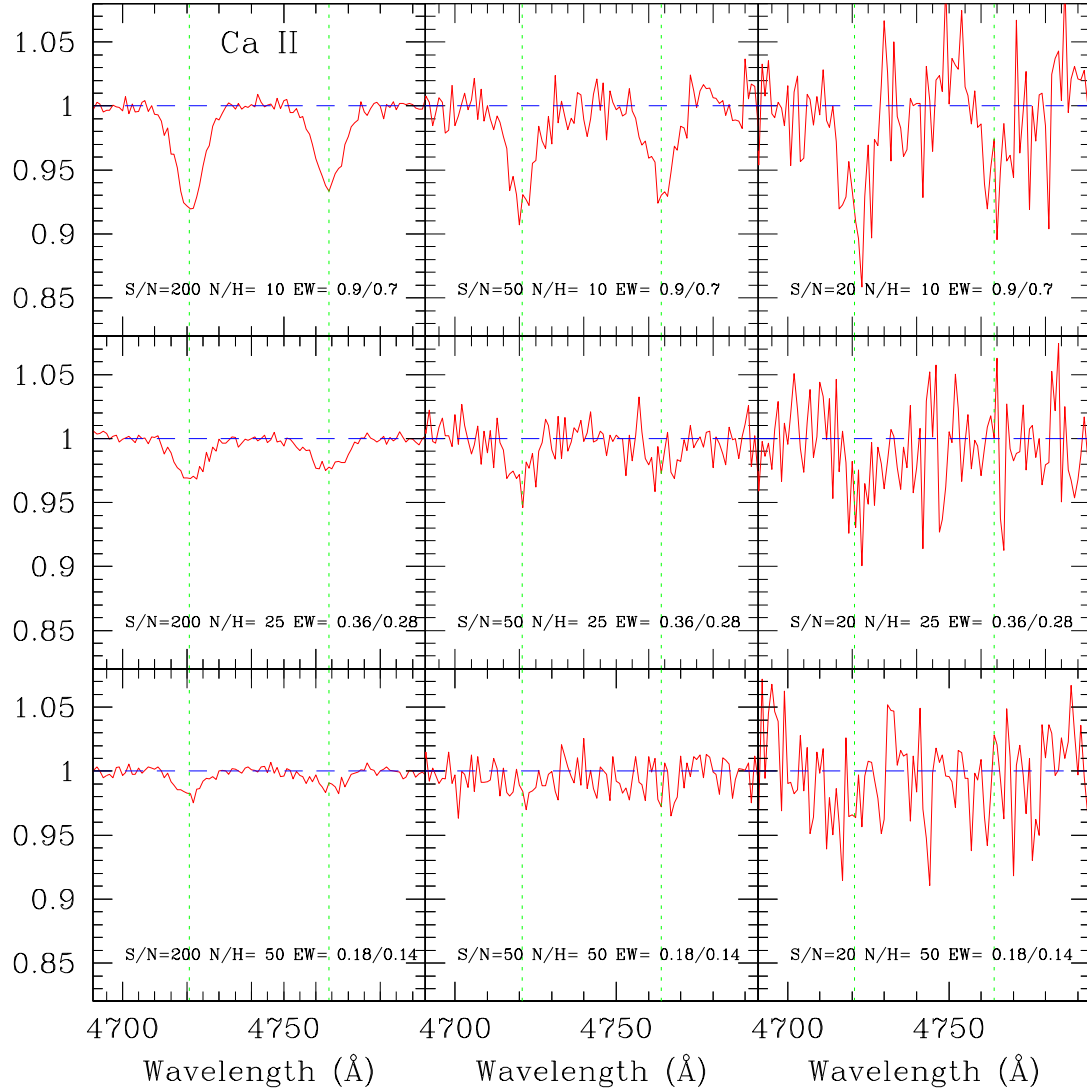


**Figure A4.** Simulation of the normalized optical spectrum of a BL Lac object at  $z = 0.2$  in the region of H, K Ca II lines. The simulation assume three different nucleus to starlight flux ratio at the observed wavelength of Ca II lines (from top to bottom) and three levels of SNR (from left to right). The two dotted vertical lines indicate the position of H, K features for reference. The horizontal dashed line gives the normalized continuum. The simulation include the statistical noise. The figure illustrate how the detectability of CaII lines depend on N/H and SNR (see also text). In each panel we give the SNR of the spectrum, the nucleus to host ratio (N/H) and the minimum EW assuming standard or 1 mag fainter host galaxy luminosity.